INVESTIGATION ON OPTICAL, DIELECTRIC AND INVITRO ANTI-INFLAMMATORY RESPONSES OF TITANIUM DIOXIDE (TiO_2) NANOPARTICLES

S. SAGADEVAN[a], Z. Z. CHOWDHURY[b,*], M. R. BIN JOHAN[b] ,
R. F. RAFIQUE[c], F. A. AZIZ[d], M. D. ENAMUL HOQUE[e],
R. SURIAKARTHICK[f]
[a]*Centre for Nanotechnology, AMET University, Chennai-603 112, India*
[b]*Nanotechnology& Catalysis Research Centre, University of Malaya, Kuala Lumpur 50603, Malaysia*
[c]*Rutgers Cooperative Extension Water Resources Program, Rutgers, The State University of New Jersey; USA*
[d]*Department of Physics, Center for Defence Foundation Studies, UniversitiPertahanan Nasional Malaysia, Kem Sg. Besi, 57000 Kuala Lumpur, Malaysia*
[e]*Department of Biomedical Engineering, Military Institute of Science and Technology (MIST)Mirpur Cantonment, Dhaka – 1216, Bangladesh*
[f]*Department of Physics, National Changhua University of Education, Changhua, Taiwan*

This article deals with synthesis of titanium dioxide (TiO_2) nanoparticles using sol-gel method. The morphological as well as optical and dielectric properties were determined. The anti-inflammatory properties of the synthesized nanoparticles were observed through in vitro assessment. For specified concentration of TiO_2 nanoparticles under restricted experimental conditions, the absorbance was measured to evaluate the anti-inflammatory property. The morphological features and particle size with their crystal structure were determined by scanning electron microscopy (SEM), transmission electron microscopy (TEM) and powder X-ray diffraction (XRD). The optical properties of TiO_2 nanoparticles were measured using UV-vis. absorption spectroscopy and photoluminescence (PL) spectroscopy. The FT-IR and Raman spectra analyses were also conducted that confirmed the presence of TiO_2nanoparticles. Under predetermined frequency and temperature level, the dielectric properties including dielectric constant, dielectric loss and AC conductivity of the synthesized TiO_2nanoparticles were determined. The findings indicated the anti-inflammatory properties of TiO_2 through in vitro assessment. The research also exhibited the inhibition of protein denaturation, protease inhibition and hemolytic assay for the synthesized Nano particles of TiO_2.

(Received April 25, 2018; Accepted July 12, 2018)

Keywords: TiO_2 nanoparticles, Photoluminescence, Anti-inflammatory, Protein denaturation

1. Introduction

Nanomaterials are chemical substances or materials which can be crystalline or amorphous and have a characteristic length scale smaller than 100 nm. Nanomaterials are known to exhibit unique characteristics compared to the same material which have increased strength, chemical reactivity or conductivity that is which does not have nano-scale features. Based on their particle size and crystallinity index, nano-particles show different structural, thermodynamic, electrical, magnetic, spectroscopic and catalytic features. Titanium dioxide (TiO_2) has drawn extensive attention because of its chemical stability, low cost and non-toxicity. However, TiO_2 is only

* Corresponding author: drzairachowdhury76@gmail.com

excited by UV light so that the efficiency of solar light is very low [1]. Titanium dioxide is chemically inert semiconductor metal oxide that displays photo-catalytic activity in the existence of light with energy equal to or greater than its band-gap energy. These unique features as well as its' relatively low price for manufacturing and processing, it is extensively used for photo-catalysis, anodic materials and dye sensitized solar cells [2-4]. Due to its' capability to give whitening effect and opacity to various products, it is widely added as additives for paints, papers and cosmetics products. The modification of nanocrystalline TiO_2, in terms of their particle sizes can significantly affect their stability and tuned their morphology based on end application [5].

Nanocrystalline titanium dioxide has carved a niche for itself under the category of promising functional materials due to its multivariant applications [6, 7], cost effectiveness, better stability towards chemical corrosion, photocorrosion and strong oxidizing power [8]. It is important to control its surface-to-volume ratio and the electronic structure which subsequently will enhance the functional properties of the nanomaterials [9]. These can be controlled by a careful selection of the method of fabrication. Among the numerous synthesis techniques, hydrothermal synthesis is considered to be more convenient because of the various advantages like particle size, morphological features, composition and phase structure can be controlled through manipulating the process variables including temperature, reaction time, pressure, concentration and pH value [10]. The sol-gel process is commonly used as it can ensure better stoichiometric ratio, low temperature for synthesis, high crystallinity values, high purity and very small particle size of the synthesized end nano materials [11-13].

There is ethical concern for conducting experimental pharmacological research using animals. Thus there is lack of knowledge for suitability of any particular methods which should be utilized. In this research, protein denaturation bioassay is selected for in vitro assessment of anti-inflammatory property of synthesized TiO_2 nanoparticles. Usually most of the proteins lose their biological functions when denatured. Due to denaturation of protein, auto-antigens are produced which causes some arthritic diseases. The mechanism of denaturation involves alteration in hydrophobic properties as well as disulphide and electrostatic hydrogen bonding [14]. Denaturation of proteins is well documented because of inflammation. The inflammatory drugs such as salicylic acid, phenylbutazone and indomethacin have shown the dose dependent ability for thermally induced protein denaturation [15]. The denaturation is the change of proteins from a soluble to an insoluble form with a large variety of chemical and physical agents including acids, alkalies, alcohol, acetone, salts of heavy metals and dyes, and heat, light, and pressure [16]. Chick and Martin considered heat denaturation as a reaction between protein and water, which implied in all probability of hydrolysis [17]. Some literature reported that denaturation of protein is one of the causes of inflmmation due to the production of auto-antigens in certain rheumatic diseases. It may be due to in vitro denaturation of proteins and proteniase. In this work, TiO_2 nanoparticles were synthesized by using sol-gel method, and the in vitro assessment of anti-inflammatory property of synthesized TiO_2 nanoparticles was conducted besides other structural and optical characterizations.

2. Experimental details

2.1 Titanium dioxide (TiO_2) nano-particles Synthesis: Titanium tetra iso-propoxide was mixed with HCl, ethanol and deionized water. It was stirred for half an hour maintaining the pH value at 1.5. After 30 minutes, 10ml of deionized water was added with the mixture and again stirred for another 2 hours at room temperature. After drying at room temperature, the powder obtained was heated at 100ºC for approximately 2 hours.

2.2 In vitro assessment of anti-inflammatory property of TiO_2 nanoparticles.

2.2.1 Inhibition of protein denaturation

Inhibition of protein denaturation was examined by the technique described in another study [18], with slight modification. Firstly, 500 µL of 1% bovine serum albumin was added to 100 µL of TiO2. This mixture was kept at room temperature for 10 minutes, followed by heating at 51°C for 20 minutes. Then the mixture was cooled down to room temperature and absorption

spectrum was recorded at 660 nm. In this process, acetylsalicylic acid was used as a positive control. The experiment was carried out in triplicates and percent inhibition for protein denaturation was calculated using following formula.

% Inhibition = $100 - [(A_1 - A_2)/A_0)*100]$

Where, A_1, A_2 and A_0 are the absorbances of sample, product control and positive control, respectively.

2.2.2 Protease inhibition assay

Inhibition of trypsin was evaluated by the method [19]. A quantity of 100 mL of bovine serum albumin was added to 100 µL of TiO_2. This mixture was incubated for 5 min at room temperature. Reaction was inhibited with the addition of 250 µL of trypsin followed by centrifugation. The supernatant was collected, and absorption spectrum was observed at 210 nm. For positive control acetylsalicylic acid is used. The experiment was carried out in triplicates and percent inhibition of protease inhibition was calculated as below.

% Inhibition = $100 - [(A_1 - A_2)/A_0)*100]$

Where, A_1, A_2 and A_0 are the absorbances of sample, product control and positive control, respectively.

2.2.3 Haemolytic assay

Haemolytic assay was carried out following the microtitre plate method [20]. In this process, the healthy human blood was collected using EDTA solution (2.7 g/100 ml) as an anticoagulant. The pellet was resuspended in normal saline (pH 7.4.) followed by three times centrifugation of as prepared mixture. Also, 1% erythrocyte suspension was prepared by adding 99 ml normal saline to 1 ml of packed RBC.

The micro haemolytic test was carried out in 96 well 'V' bottom micro titer plates. Different rows were selected for the different samples. In all the wells the serial dilution of the crude extracts (100 µl) was done till the last well, and 100 µl was discarded from last well. 1% RBC (100 µl) was added into all the 96 wells with standard controls that were included in the test. 1% RBC suspension, 100 µl of distilled water was added, which acted as a positive control and 100 µl of normal saline, which acted as negative control. The results were recorded after 3 hours stand of plate at room temperature. The red color suspension in the wells considered as positive haemolysis and button formation at the bottom of the wells was considered as lack of haemolysis.

2.3 Characterizations Techniques

The XRD pattern of the TiO_2 powder was measured using a powder X-ray diffractometer (Schimadzu model: XRD 6000 using CuK_α with a diffraction angle between 20° and 70º). For morphological study, scanning electron microscopy (SEM) (JEOL, JSM- 67001) and transmission electron microscopy (TEM) (H-800 TEM, Hitachi, Japan) with an accelerating voltage of 100 kV were used. UV-Vis. absorption spectra for the TiO_2 nanoparticles were recorded using a Varian Cary 5E spectrophotometer in the range of 200-1000 nm. The thin film surface morphology's evaluated by contact mode atomic force microscopy (AFM Multimode 8, Bruker). The FT-IR spectrum of the TiO_2 nanoparticles was recorded using an FT-IR (Bruker IFS 66W) spectrometer. Raman spectrum was collected using a Bruker RFS 27: stand-alone model Raman spectrometer. The photoluminescence (PL) spectra of the TiO_2particles were recorded by Perkin-Elmer lambda 900 spectrophotometer with a Xe lamp as the excitation light source. The dielectric properties such as dielectric constant and dielectric loss of TiO_2 nanoparticles were investigated by using an HIOKI 3532-50 LCR HITESTER with frequency range 50Hz-5MHz.

3. Results and discussion

3.1. Structural and optical properties

In the present work, XRD was carried out over the synthesized TiO_2 nanoparticles with CuK_α radiation. Fig.1 demonstrates that the diffraction peaks appear for the planes of (101), (004), (200), (105) and (204). The peaks indicate the formation of anatase phase of TiO_2. The synthesized

material i.e TiO_2nanoparticles displays a tetragonal structure. The average grain size (D) was calculated using the Scherrer formula [21].

$$D = \frac{0.9\lambda}{\beta \cos\theta} \tag{1}$$

where, λ is the X-ray wavelength, θ is the Bragg diffraction angle, and β is the FWHM of the XRD peak appearing at the diffraction angle θ. The average grain size of TiO_2nanoparticles at most prominent peak at (101) is found to be around 14 nm.

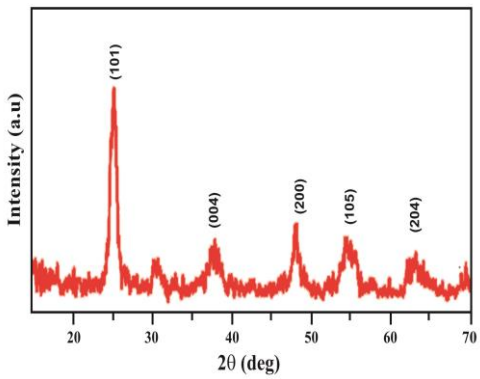

Fig.1.X-ray diffraction (XRD) pattern of as prepared TiO_2 nanoparticles

The surface morphology of the synthesized TiO_2 nanoparticles is analyzed by SEM and is illustrated byFig.2 (a-f).The SEM images (Fig.2 (a-f)) revealed fairly uniform distribution of TiO_2 nanoparticles. From the SEM images (Fig.2 (a-c)), it is observed that most of the grains fall in the nanoscale regime. It is also noted that the particles get aggregated on their surface. Aggregation of particles on the surface might be originated from the high surface energy of the synthesized nanoparticles as displayed in Fig.2 (a-c).SEM images (Fig.2 (e-f)) show particle heterogeneous, spherical and elongated, with large particle size distribution. From the micrograph it is clearly seen that the particles are spherical shape and uniformly distributed. Larger particles in this figure may be aggregates of the smaller particles (Fig.2 (a-c)). The value of particle size observed from SEM was in good agreement with the results obtained from XRD. The average grain size was found to be 12 nm.

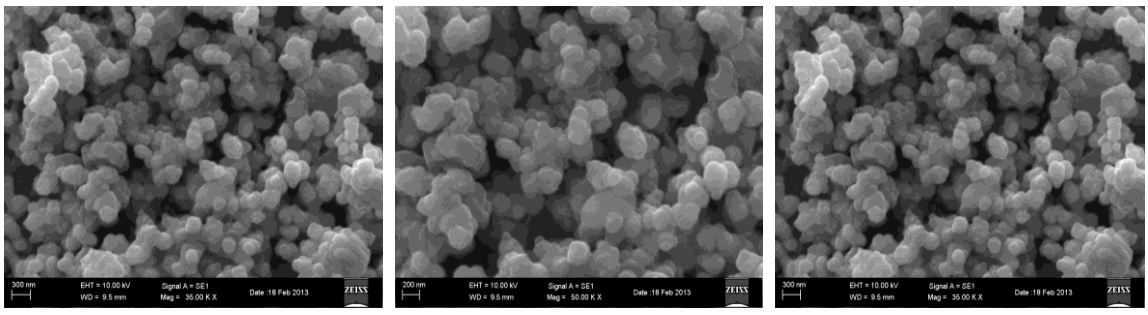

Fig.2.1. SEM images of uniformly distributed TiO_2 nanoparticles at:
(a) 300nm) (b) 200 nm) (c) 100nm

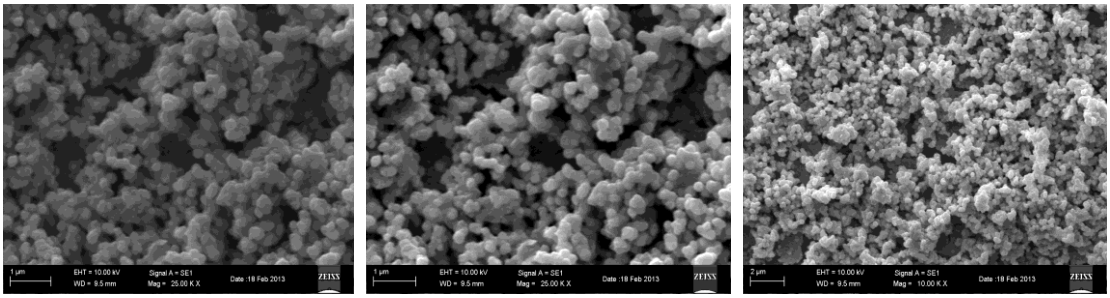

Fig 2.2. SEM images of uniformly distributed TiO_2 nanoparticles at 1μm

TEM is commonly used for imaging and analytical characterization of the nanoparticles to assess the shape, size, and morphology. TEM images of the TiO_2 nanoparticles are shown in Fig.3 (a-d). It is evident from the Fig.3 (a-d) that the particles were smaller in size and uniform in shape. The estimated particle size was around 22 nm. The Fig.3 (e) shows the HRTEM image of TiO_2 nanoparticles with an interplanar spacing of 0.30 nm which corresponds to the separation between the (101) lattice planes of TiO_2. The diffraction rings from selected area diffraction pattern (SAED) image (fig.3 (f)) are indexed to the (101), (004), (200), (105) and (204) planes of tetragonal phase, which matched with the XRD data.

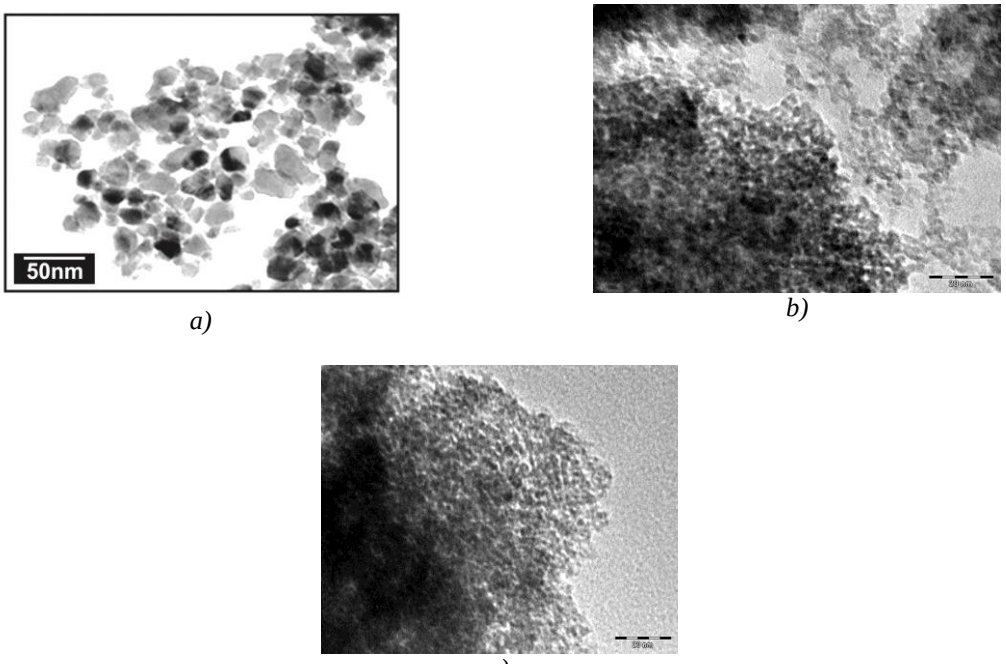

a) *b)* *c)*

Fig.3.1. TEM images of TiO_2 nanoparticles (a) 50 nm; (b) 40 nm: (c) 30 nm

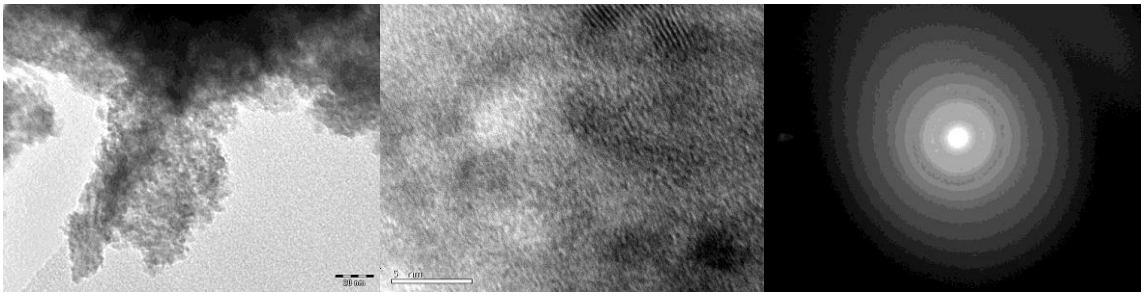

Fig.3.2. HR-TEM images of TiO_2 nanoparticles (d) 20nm; (e) 5nm: (f) SAED Pattern of TiO_2

The FT-IR spectrum of TiO_2 nanoparticles is shown in Fig.4. Peaks at 3450 cm^{-1}, 3375 cm^{-1}, and 3262 cm^{-1} correspond to stretching vibration of the O-H bond. Peak observed at 2925 cm^{-1}, 1656 cm^{-1} corresponds to the C-H stretching vibration adsorbed H_2O, respectively. The peaks at 1394 cm^{-1} and 1155 cm^{-1} correspond to C-O vibrations. The peaks observed at 620 cm-$^{-1}$, 590 cm^{-1}, and 540 cm^{-1} correspond to Ti-O vibrations. The peak between 800 and 400 cm^{-1} is assigned to the Ti-O stretching bands. The evidenced peak broadening can be ascribed to the small size of the prepared samples. TiO_2 exhibited the characteristic peaks corresponds to the anatase phase with the absence of secondary or impurity peaks. Fig.5 shows FT-Raman spectra of the as prepared titanium dioxide (TiO_2) nanoparticles. The characteristic high frequency Raman mode of anatase phase was observed for the peaks at 405, 530, and 650 cm^{-1}.

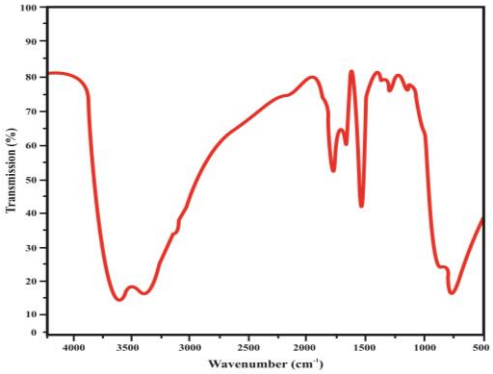

Fig. 4.FT-IR spectrum of TiO_2 nanoparticles

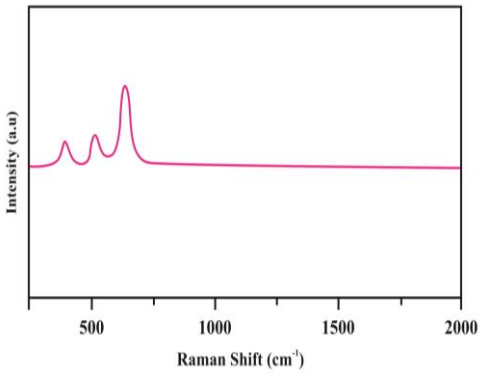

Fig.5. Raman spectrum of TiO_2nanoparticles

The characteristics of the band structure of the materials can be observed from optical adsorption studies. Fig.6 shows wavelength of the as prepared TiO_2 nanoparticles with the variation in optical absorbance. The optical absorption coefficient was calculated in the wavelength range of 200 - 1000 nm. Further, at higher wavelengths the samples were found to be completely transparent. The absorption band edges were estimated to be around 355 nm. The increments in absorption of TiO_2nanoparticles with respect to control indicated a stabilization of protein, i.e. inhibition of protein (albumin) denaturation or anti-denaturation effect by the test extract. The peak broadening of the absorption spectrum could be because of quantum confinement of the nanoparticles.

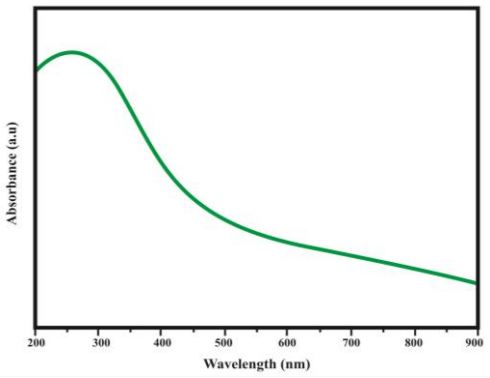

Fig.6. UV-visible absorption spectrum of TiO_2 nanoparticles

The study has an absorption coefficient (α) obeying the following relation for high photon energies (hν) as follows;

$$\alpha = \frac{A(h\nu - E_g)^n}{h\nu} \quad (2)$$

Where, α,A *and* E_g are the absorption coefficient, constant and band gap, respectively. The fundamental absorption corresponding to the optical transition of the electrons from the valence band to the conduction band can be used to determine the nature and value of the optical band gap Eg of the nanoparticles. The exponent 'n' depends on the type of transition and it may have values 1/2, 2, 3/2 and 3 corresponding to the allowed direct, allowed indirect, forbidden direct and forbidden indirect transitions, respectively. The band gap is determined by extrapolating the linear portion of the curve. The direct band gap energies were calculated by plotting Tauc's graphs between $(\alpha h\nu)^2$ versus photon energy (hν) for TiO_2 nanoparticles is shown in Fig.7. The intercept of the tangent to the plot on the X-axis gives the direct band gap of TiO_2 nanoparticles. The band gap was found to be 3.2 eV. The calculated band gap energy for the prepared TiO_2 nanoparticles is higher than the bulk material. This is due to the quantum confinement effect. The reduction in particle sizes results in increase of surface/volume ratio. Surface atom has lower coordination number and atomic interaction which increases the highest valance band energy and decreases the lowest unoccupied conduction band energy. This leads to increase in band gap.

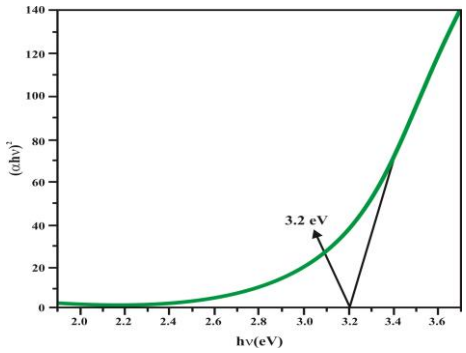

Fig.7.Evaluation of $[(\alpha h\nu)^2]$ plotted against photon energy (h ν) of the optical energy band (E_g) diagram of TiO_2 nanoparticles.

PL spectra were recorded for the sample synthesized with the wavelength range of 300-500 nm and is illustrated by Fig. 8. From Fig. 8, it could be observed that at room temperature the emission band is centered on at 390 nm. It has been reported that nanostructured titania generally exhibits a broad emission band centered at around 360-500 nm at room temperature [22]. This phenomenon is attributed to the surface defects. Basically this plays a major role in defining the

luminescence properties. The peak in the photoluminescence spectrum between 320-400 nm indicates to the direct recombination between electrons and holes [23].

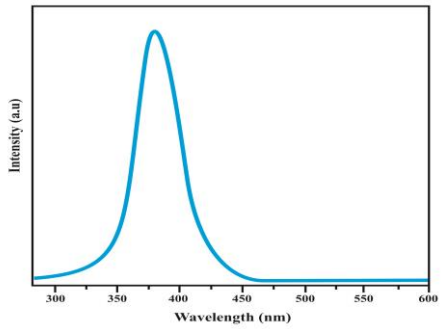

Fig.8.Photoluminescence spectrum for TiO_2 nanoparticles

The dielectric loss and dielectric constant of the pellets of TiO_2 nanoparticles were measured using disk form for different frequencies under predetermined range of temperatures. The deviations in dielectric constant at different frequency and temperature range for TiO_2 nanoparticles are illustrated by Fig.9.

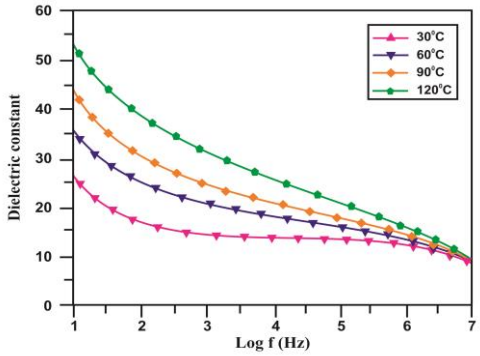

Fig.9 Variation of dielectric constant with frequencies at different temperatures

The magnitude of dielectric constant was high in the lower frequency region. This is caused by the presence of all four polarizations namely, space charge, orientations, electronic, and ionic polarization and it decreases with the increase of frequency [24]. From the plot, it revealed that dielectric constant increases with increasing temperature. This occurs due to the presence of space charge polarization near to the grain boundary interfaces. However, this factor is completely dependent on the perfection and purity of the synthesized sample [25]. The variations in dielectric loss of TiO_2 nanoparticles against temperature and frequency are illustrated by Fig.10. It can be observed that the magnitude of dielectric loss is inversely proportional to value of frequency. Approximately at higher frequencies, the magnitude of loss angle has the same value at all temperature range studied here. Due to presence of adsorption current in dielectric materials, dielectric losses occur. In case of polar dielectric materials, the orientation of molecules along the direction of the external electric field needs adequate electric energy. This energy is needed to overcome the forces of the internal friction [26].

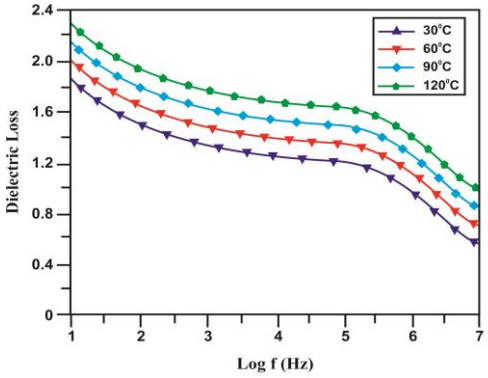

Fig.10.Variation of dielectric loss with frequencies at different temperatures

The phenomenon of space charge formation as well as inhomogeneity analogues to defects inside the inter phase layers causes absorption current. Subsequently this causes the dielectric loss in nano-materials [27]. The AC electrical conductivity of TiO_2 nanoparticles is illustrated by Fig.11.

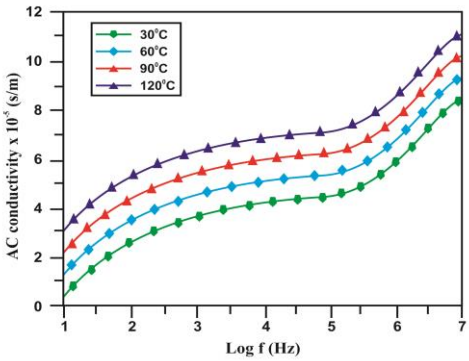

Fig.11. AC conductivity of TiO_2nanoparticles

It was observed that the magnitude of AC electrical conductivity is proportional with frequency level. Due to increase of hopping frequency of electrons at higher frequency level, the AC conductivity of the material was also increasing at higher frequency level [28]. With increase in temperature, the grain size of the particles usually increases resulting decrease in grain boundaries. Thus, conductivity increases with increased rate of conduction losses. For small polaron hoping, usually high AC conductivity is observed at higher frequencies [29]. The conductivity of nanomaterials is caused by highly localized charge carriers bound to the lattice with lattice strain which is known as polaron conduction [30, 31].

3.2. Anti-inflammatory property of TiO_2 nanoparticles

In this study, the ability of TiO_2 to inhibit protein denaturation was studied. Selected extracts were effective in inhibiting heat induced albumin denaturation. TiO_2 was observed as 68.92% µg/mL and respectively. Aspirin was used as a standard anti-inflammation drug. Results are presented in Fig. 12.TiO_2 exhibited significant antiproteinase activity. The percentage of inhibition was observed in TiO_2. The standard aspirin 72.9% drug showed maximum proteinase inhibitory action. TiO_2 was observed as crude extraction 66.9% µg/mL. Results are shown in Fig.13.

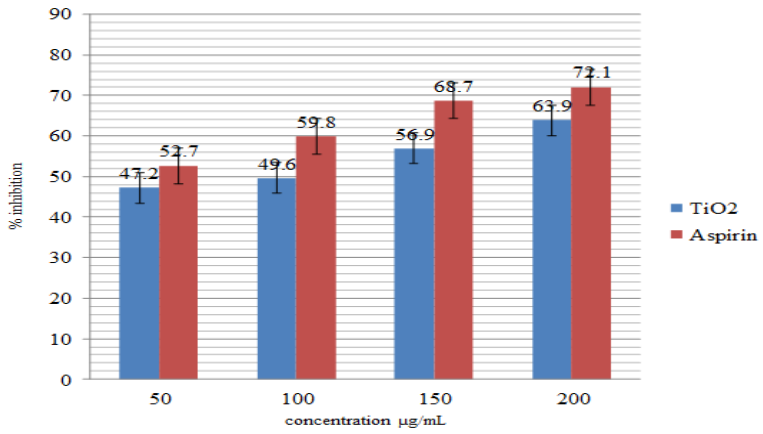

Fig.12.Inhibition of protein denaturation activity

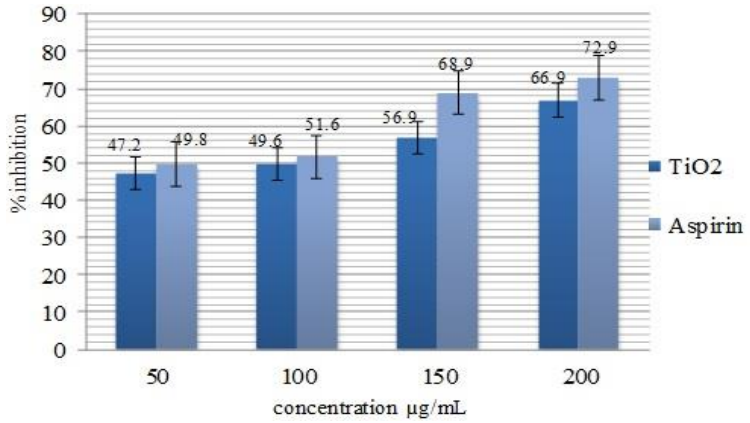

Fig.13.Inhibition of proteinase activity

In haemolytic assay, haemolytic activity of the TiO_2 is 32 HU. The Present study supports the previous reports, i.e. the hemolytic activity of TiO_2, Halocynthiaaurantium disrupted 8% and 16% of human erythrocytes, respectively [32]. Hemolysis of human and sheep red blood cells has been studied by Al-Hassan et al. [33]. Al-Lahham et al. has studied the specific activity of the catfish epidermal factor reporting to be of 20.6 units mg^{-1} protein, which is found to be a level somewhat lower than that of most protein hemolytic factors [34].

4. Conclusions

In this work, sol-gel method was used to synthesize the TiO_2 nanoparticles successfully. The X-ray diffraction (XRD) pattern confirmed the formation of TiO_2 nanoparticles. The surface morphological studies from SEM analysis illustrated the spherical shape of the synthesized TiO_2nanoparticles; whereas TEM analysis determined the particle size of the as synthesized TiO_2 nanoparticles. The particle size determined was around 22 nm. FT-IR and FT-Raman spectra confirmed the presence of functional group in the synthethesized TiO_2 sample. The UV-Vis. absorption spectrum measured the band gap value to be of 3.2 eV. The PL spectrum identified that the prepared TiO_2 nanoparticles exhibited the broad emission at 390 nm. The dielectric constant, the dielectric loss and AC conductivity were also evaluated at different frequency level and temperature range. The TiO_2 nanoparticles exhibited significant antiproteinase activity. The standard aspirin 72.9% drug showed maximum proteinase inhibitory action. The TiO_2 was observed as crude extraction 66.9% µg/mL respectively. The in vitro anti-inflammatory

assessment evidenced that the TiO_2nanoparticles prevented protein denaturation. The preliminary results of this study suggest that the synthesized TiO_2 nanoparticles have high potential in anti-inflammatory drug development. However, further definitive in vivo studies are necessary to ascertain the detail mechanisms and constituents of TiO_2 necessary for its anti-inflammatory action, which is aimed in our further follow up study.

Acknowledgements

This work has been made possible because of the generous grants RP044C-17AET and RP044D-17AET from the University Malaya, Malaysia. One of the authors (Suresh Sagadevan) acknowledges the honor, namely the "Visiting fellow" at the Department of Physics, Center for Defence Foundation Studies, Universiti Pertahanan Nasional Malaysia, Kem Sg. Besi, 57000 Kuala Lumpur, Malaysia. The author wishes to place on record his heartfelt thanks that are due to the authorities concerned.

Conflict of Interest

All the authors declare that there is no conflict of interests.

References

[1] T. Morikawa, R. Asahi, T. Ohwaki, A. Aoki, Y. Taga, Jpn. T. Appl. Phys. **40**, L561 (2001).
[2] M.R. Hoffmann, S.T. Martin, W. Choi, D.W. Bahnemann, Chem. Rev.**95**,69 (1995).
[3] D.L. Liao, B.Q. Liao, J. Photochem. Photobiol. A: Chem, **187**,363 (2007).
[4] K. Shankar, J. Bandara, M. Paulose, H. Wietasch, O.K. Varghese, G.K. Mor, T.J.LaTempa, M. Thelakkat, C.A. Grimes, Nanoletters**8**,1654 (2008).
[5] H. Zhang, J. F. Banfield, J. Mater. Chem.**8**,2073 (1998).
[6] X.H.Xia, Y.S. Luo, Z.Wang, Y.Liang, J. Fan, Z.J.Jia, Mater. Lett.**61**,257-4 (2007).
[7] I.D.Kin, A.Rothschild, B.H.Lee, D.Y.Kim, S.M.Jo, H.L.Tuller, Nano Lett.**6,**2009-13 (2006).
[8] M.R. Hoffmann, S.T. Martin, W. Choi, D. W. Bahnemann, Chem. Rev.**95**, 69 (1995).
[9] M. Tomita, M. Matsuoka, Masahiro, J. Opt. Soc. Am.**B7**, 1198 (1990).
[10] K. Byrappa, M. Yoshimura, Handbook of Hydrothermal Technology, William Andrew Publishing, New York, 2001.
[11]V.R.Gonzalez,M.A.R.Gomez,L.M.T.Martinez,R.Gomez,Top Catal. **54**, 490 (2011).
[12] K.S.Hwang, J.H.Jeong, J.H. Ahn, B.H.Kim, Ceram. Int.**32**,935 (2006).
[13] Suresh Sagadevan, American Journal of Nanoscience and Nanotechnology**1**, 27 (2013).
[14] M. L.Anson, A. E.Mirsky, Gen Physiol.**15**, 341 (1932).
[15] C. T.Chou,Phytother Res. **11**, 152 (1997).
[16] T. B. Robertson, The physical chemistry of the proteins, New York and London. 1918.
[17] J. R.Vane,R, M.Botting, Inflammation Research. **44**(1), 1 (1995).
[18] Y.Mizushima, M.Kobayashi, J.Pharm.Pharmacol. **20**(3), 169 (1968).
[19] S.Sakat, A. R.Juvekar, M. N. Gambhire, Int. J. Pharm. Pharm. Sci. **2**(1), 146 (2010).
[20] K. PaniPrasad, K.Venkateshvaran, Central Institute of Fisheries Edu. (pp. 41). India (1997).
[21] A. L. Patterson, Phys. Rev. **56**, 978 (1939).
[23] Y. Lei, D. Zhang, J. of Materials Research**16**,1138 (2001).
[24] J. Liqiang, S. Xiaojun, X. Baifu, W. Baiqi, C. Weimin, F. Honggang, Journal of Solid State Chemistry **177**,3375(2004).
[25] S. Suresh, C. Arunseshan, ApplNanosci.**4**,179 (201).
[26] Sagadevan Suresh, ApplNanosci. **4**, 325 (2014).
[27] Suresh Sagadevan,JibanPodder, International Journal of Nanoparticles **8**(3/4),289 (2015).
[28] Sagadevan Suresh, International journal of Physical Sciences. **8**, 1121 (2013).

[29] K.T. Selvi, K.A. Mangai, M. Priya, M. Rathnakumari, P. Sureshkumar, S. Sagadevan, Nanomater.Nanotechnol.**6**, 1(2016).
[30] S. Suresh, C. Arunseshan, Appl. Nanosci. **4**, 179 (2014).
[31] Suresh Sagadevan, Kaushik Pal, P. Koteeswari, A. Subashini, J Mater Sci: Mater Electron DOI 10.1007/s10854-017-6488-3 (2017).
[32] K. L. Jang, W. J. Livesley, P. A. Vernon. Twin Research.**5**(5),342 (2002).
[33]J.M.Al-Hassan, M. Thomson, R. S. Criddle, Mar. Biol.**70**, 27(1982).
[34] A.Al-Lahham, J.M. Al-Hassan, M. Thomson, R.S. Criddle, Comp. Biochem. Physiol.**87B**, 321(1987).